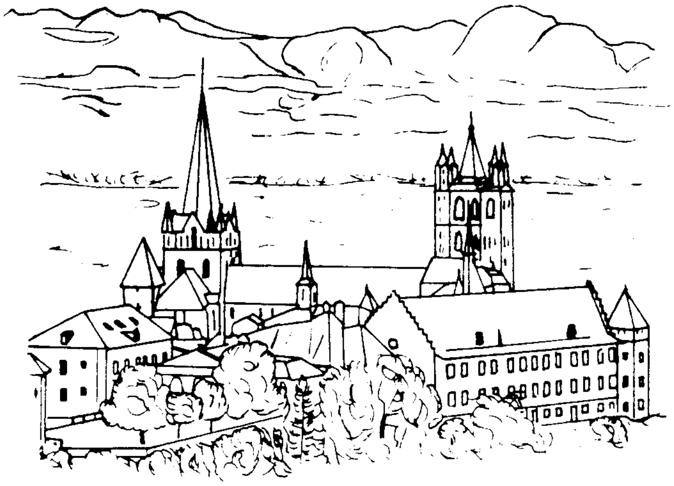

1984 INTERNATIONAL CONFERENCE ON PLASMA PHYSICS

Lausanne - Switzerland June 27 - July 3, 1984

PROCEEDINGS CONTRIBUTED PAPERS

Volume I

Editors: M.Q. Tran, M.L. Sawley - CRPP-EPFL, 21, av. des Bains
CH-1007 Lausanne / Switzerland

CENTRE DE RECHERCHES EN PHYSIQUE DES PLASMAS
ECOLE POLYTECHNIQUE FEDERALE DE LAUSANNE

EXCITATION OF ION AND PLASMA WAVES BY LASER BEAMS

Francis F. Chen, B. Amini, C. E. Clayton, and H. C. Barr*
University of California, Los Angeles, California 90024

Abstract: The intricate nature of stimulated scattering processes in laser-plasma interactions is revealed in experiments and calculations.

1. Saturation of SBS by Ion Trapping[1] (Clayton)

Experiments on stimulated Brillouin scattering (SBS) of CO_2 laser light in plasma targets have shown a saturation plateau at a power reflectivity level R of < 10%. To understand this, we have probed the excited ion wave by ruby laser Thomson scattering; the scattered light is resolved in frequency and angle and is streaked in time. Harmonics of the ion wave are seen without turbulence (Fig. 1), but these have the same threshold and growth rate as the fundamental and are therefore unlikely to cause saturation. Streak pic-

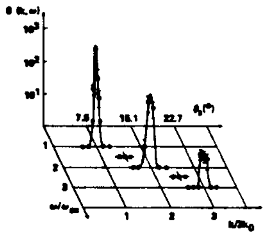

Fig. 1

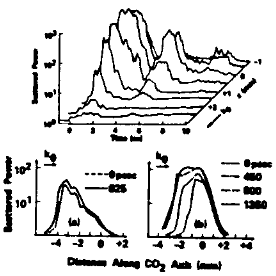

Fig. 2

tures yield the spatial structure of the ion wave pulsations (Fig. 2). At low power, the ion wave grows exponentially toward the pump (Fig. 2a). At high power, the wave develops a flat top (Fig. 2b) at n_1/n_o = 5-10%, corresponding to the measured R of 6%. The wave saturation level can be explained quantitatively by the nonlinear frequency shift caused by trapped ions; the wave gets out of phase with the pump and stops growing. The length of the flat top increases with power. The onset of deep trapping depends on the rate of diffusion in velocity space out of the trapping zone (Fig. 3). Taking into account that $\Delta v_\perp > \Delta v_{||}$ and averaging over angles and velocities, we obtain a trapping threshold consistent with the saturation level.

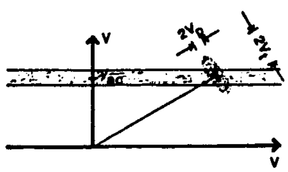

Fig. 3

2. Observation of the Raman Threshold (Amini)

To clarify possible misunderstanding of the SRS threshold, we have recalculated the spatial growth rate κ in a finite, homogeneous plasma:

$$\kappa = -B + (B^2 + 4C)^{1/2}, \qquad (1)$$

where

$$B = \frac{1}{2}\left(\frac{\gamma_1}{V_1} + \frac{\gamma_2}{V_2}\right) \quad \text{and} \quad C = \frac{\gamma_o^2 - \gamma_1\gamma_2}{V_1V_2},$$

$\gamma_{1,2}$ and $V_{1,2}$ being the damping rates and group velocities of the plasma and backscattered waves, respectively, and γ_o is the homogeneous growth rate. When the homogeneous threshold $\gamma_o^2 > \gamma_1\gamma_2$ is exceeded, κ is positive. In a finite length L, the condition $\kappa L >> 1$ requires $\gamma_o^2 >> \gamma_1\gamma_2$ and $4C > B^2$; this leads to the usual "absolute" threshold

$$\gamma_o > \frac{1}{2}\left(\frac{\gamma_1}{V_1} + \frac{\gamma_2}{V_2}\right)(V_1V_2)^{1/2}. \qquad (2)$$

When this is well satisfied,

$$\kappa \approx 2C^{1/2} \approx \gamma_o(V_1V_2)^{-1/2}. \qquad (3)$$

An inhomogeneous plasma can be treated by using for L the distance between turning points. For a density scalelength L_n, this turns out to be

$$L = (12k_1L_n\lambda_D^2)^{1/2} \text{ (linear profile)} \qquad (4)$$

$$L = (18k_1L_n^2\lambda_D^2)^{1/3} \text{ (parabolic profile)} \qquad (5)$$

For $\kappa L >> 1$, Eqs (3) and (4) yield the usual inhomogeneous threshold $v_o^2/c^2 >> 1/k_oL_n$, while Eqs. (3) and (5) give for the parabolic case $v_o^3/c^3 >> (32/3)^{1/2}(\lambda_D/L_n)/k_oL_n$, remarkably close to the "exact" solution.[2] In practice, however, the B^2 term in Eq. (1) cannot be neglected even though Eq. (2) is satisfied. Requiring $\kappa L >> 1$ and expanding the square root, we obtain the more severe criterion

$$\gamma_o^2 L/c\gamma_1 >> 1. \qquad (6)$$

This has the same form as that used for SBS, but L is to be found from Eq. (4) or (5).

The SRS threshold has been measured for the first time in a plasma where SBS cannot and does not occur: a theta-pinch with $T_i >> T_e$. The apparatus is shown in the right half of Fig. 4. The growth curve (Fig. 5) shows a threshold of $\approx 5 \times 10^{10}$ W/cm^2. This value agrees with Eq. (2), but only by accident. The correct threshold, Eq. (6), is about ten times higher. The discrepancy is unexplained, but filamentation is an obvious possibility.

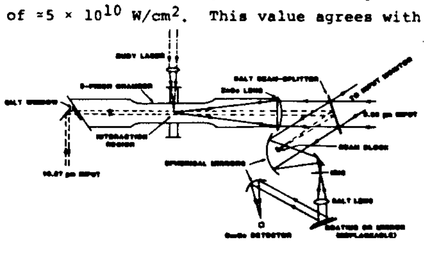

Fig. 4

3. Excitation and Detection of Plasma Waves with Lasers (Amini)

Plasma waves have been excited by optical mixing of two opposing laser beams of 9.56 and 10.27 μm wavelength in a theta-pinch plasma (Fig. 4). The 5-μm wavelength plasma waves are detected by ruby-laser Thomson scattering along a perpendicular axis. Fig. 6a shows the spectrum of scattered ruby light at high gain when only one CO_2 beam is present below SRS threshold. The peak due to hyperthermal plasma waves gives the Bohm-Gross frequency ω_{BG} directly. (The right-hand portion has been attenuated to show the unshifted peak.) When optical mixing occurs, the plasma wave peak increases 35 times, as shown in Fig. 6b (reduced gain, with the peak downshifted to bring it on-scale). This occurs only when the plasma density is resonant ($\approx 6 \times 10^{16}$ cm^{-3}); that is, when ω_{BG} matches the beat frequency of the two pumps. The resonance is shown on Fig. 7.

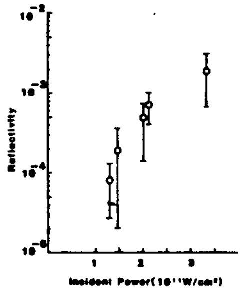

Fig. 5

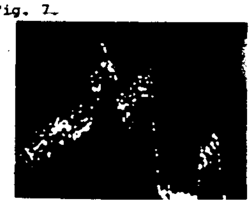

Fig. 6a

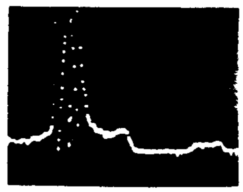

Fig. 6b

4. Raman Instability in a Density Ripple (Barr)

Since SRS usually has a higher threshold than SBS, the density inhomogeneity to be overcome in SRS is likely to be the ion wave excited by SBS. This can be considered an $\omega \approx 0$ density ripple with a wavenumber k_i slightly larger than that (k_e) for the plasma wave. In an underdense plasma, $k_i \approx k_e \approx 2k_o$, and $\Delta k \equiv k_i - k_e \approx \omega_p/c$. The ripple mode-couples the directly driven mode k_e to harmonics with $k = k_e + nk_i$, (n = 1,2,3...) to a long-wavelength mode with n = -1, k = -Δk, and to backward modes with $n = -2,-3,\ldots$ The mode coupling is described by the Mathieu equation, and Landau damping causes a natural truncation of the high-n modes. A kinetic calculation shows that the lowest three modes ($k = k_e$, $k = -\Delta k \approx 0$, $k = k_e - 2k_i \approx -k_e$) are closely coupled and can have comparable magnitudes regardless of which one is driven, depending on the parameters. For example, Fig. 8 shows the k-spectrum for a new eigenfrequency that arises with ripple, in this case, one of 18%. This mode has a large component at $k = -\Delta k$ which can accelerate trapped electrons to the high velocity usually associated with Raman forward scatter.

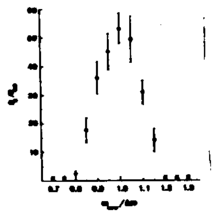

Fig. 7

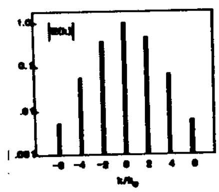

Fig. 8

5. Detection of Instabilities by Stark Satellites (Amini)

The detection of excited wave frequencies in a small focal region is a difficult experimental problem. We show evidence of a possible new technique. Fig. 9 shows the Stark broadened allowed line of ionized He at 4686 Å emitted from a theta-pinch with $n \approx 5 \times 10^{16}$ cm^{-3}, $T_e \approx 15$ eV. Subsidiary peaks equally spaced at 60 GHz can be seen. The frequency corresponds to the electron cyclotron frequency, and may indicate the existence of electron Bernstein waves in the theta-pinch. There was no laser excitation in this experiment.

Fig. 9

This work was supported by the National Science Foundation and the Lawrence Livermore National Laboratory. One of us (H.C.B.) thanks Prof. F. F. Chen for hospitality during a stay at UCLA.

REFERENCES

* Permanent address: University College of North Wales, Bangor, U.K.

1. C. E. Clayton, C. Joshi, and F. F. Chen, Phys. Rev. Letters 51, 1656 (1983) and Laser Interaction and Related Plasma Phenomena, Vol. 6, p. 621 (1984); C. E. Clayton, Thesis, UCLA PPG-759 (1983).

2. C. S. Liu, M. N. Rosenbluth, and R. B. White, Phys. Fluids 17, 1211 (1974).